IOP Conf. Series: Materials Science and Engineering **408** (2018) 012028 doi:10.1088/1757-899X/408/1/012028

The Influence of Blade Tip Loading Distribution on the Performance of a High Loading Centrifugal Impeller

Yilin Wang [1], Zefeng Li[1], Donghai Jin [1,2,*] and Xingmin Gui [1,2]

[1] School of Energy and Power Engineering, Beihang University, Beijing, China
[2] Collaborative Innovation Center For Advanced Aero-engine, Beijing, China

[*]jdh@buaa.edu.cn

Abstract. It has been proved that different blade loading distributions between tip and hub has a significant effect on centrifugal impeller performance, but the effect of loading difference at different location along the stream has not been fully understood. In this paper, several blades were modelled by a three-dimensional inverse design method, in which the impellers are defined by the blade loading distribution at its tip and hub and the flows are computed numerically by a commercial CFD code. Firstly, two impellers were modelled using the same distribution at the hub but giving different distributions at tip. The results show that the impeller with a smoother tip loading distribution performs better. At design flow rate, the total pressure ratio is found to be 1.8% higher and the efficiency rises 1.36% as well. Then a further research about the effect of increasing tip load at different parts along the flow path was carried out. Further analysis indicates that adding the load at the fore part of tip could increase the efficiency at design flow rate and brings more uniform impeller exit flow. However, the surge margin was narrowed by such change. Besides, adding the v_ur at the aft part of tip will promote the pressure ratio, with no adverse effect on the stable operation range.

1. Introduction

Different from axial compressors, centrifugal compressors always possess a more complicated three-dimensional flow structure. Due to the narrow flow channel, large streamline curvature, and the Coriolis force, inevitable severe secondary flow happens in the impeller, which leads to a pitchwise non-uniform impeller exit flow. As a consequence, the flow in radial diffuser is always coupled with a considerable loss. Therefore, impeller design has always been a difficult part in the design process of centrifugal compressors.

At present, the inverse method of blade loading control has become a key technique in modern impeller design process. M.Zangeneh [1-3] developed a set of guidelines for the suppression of secondary flows. Therefore, a loading distribution in which the maximum loading is set in the fore part of the impeller at the shroud and the aft part at the hub has been applied in several different centrifugal pump impellers. As a result, the performance of the impeller designed using these guidelines was found to be 5 percent higher at the peak efficiency point as compared to the corresponding conventional impeller. Jiancheng Shi et al. [4] applied three kinds of loading distributions in a transonic impeller and demonstrated that the aft-loading impeller achieves the best performance. Lihua Tao [5] investigated the effects of different blade loading distributions on aerodynamic performance of a subsonic centrifugal impeller and stated that higher design efficiency can be obtained with fore-loading on the shroud and aft-loading on the hub, but the surge margin was narrowed. H F Leng [6]

Content from this work may be used under the terms of the Creative Commons Attribution 3.0 licence. Any further distribution of this work must maintain attribution to the author(s) and the title of the work, journal citation and DOI.
Published under licence by IOP Publishing Ltd

also made a similar conclusion in a double suction centrifugal pump. Manabu Yagi [7] thinks that the relative velocity decelerates with regards to the enhance of load at the fore part of tip, thus the flow separation at the axial to radial turning is controlled.

It is clear that the blade loading distribution has a significant influence on the performance of centrifugal impellers. Notably most of the past research objects were subsonic, low specific speed impellers with a relatively small flow coefficient and usually the loading distributions were totally changed. Actually impellers perform remarkably different along the load variation of tip even they adopt a similar kind of loading distribution. Besides, the increase of load in different parts of tip also works in different ways. In this paper, a CFD method is adopted to a high flow coefficient, high load, low specific speed transonic impeller to analyze the effect of different tip loading distribution on the performance.

2. The effect of blade loading distribution on the flow

The inverse design method based on a inviscid streamline curvature method procedure is developed by Ji Guofeng[8], where the meridional parameter v_ur is specified as a design input. This parameter directly represents the amount of work done by the blades on flow, which was defined as ℓ_u:

$$\ell_u = \omega(v_{u2}r_2 - v_{u1}r_1) \tag{1}$$

Where v_u is the circumferential component of absolute speed v, r the radius. On the other side, ℓ_u could also be written as:

$$\ell_u = \frac{1}{2}(v_2^2 - v_1^2) + \frac{1}{2}(w_1^2 - w_2^2) + \frac{1}{2}(u_2^2 - u_1^2) \tag{2}$$

Where u means rotation speed, w represents the relative speed in rotating coordinate. Combined with the energy equation:

$$\ell_u = \frac{1}{2}(v_2^2 - v_1^2) + \int_1^2 \frac{1}{\rho} dp + \ell_f \tag{3}$$

It can be derived that:

$$\frac{1}{2}(w_1^2 - w_2^2) = \frac{1}{2}(u_1^2 - u_2^2) + \int_1^2 \frac{1}{\rho} dp + \ell_f \tag{4}$$

It can be considered that a higher v_ur leads to an increase of v, a decrease of w, and an increase of static pressure. A higher static pressure gradient from tip to hub helps controlling the secondary flow of the blade surface, which can be easily seen from the conservation equation of the momentum in inviscid flow:

$$(\boldsymbol{W} \cdot \nabla)\boldsymbol{W} + 2\boldsymbol{\omega} \times \boldsymbol{W} = -\frac{1}{\rho}\nabla p + \nabla\left(\frac{u^2}{2}\right) \tag{5}$$

For the secondary flow within the boundary layer of the impeller, static pressure gradients and centrifugal force are the main factors driving radial migration. Adopting a higher v_ur at tip than hub increases the static pressure gradient, which in turn supresses secondary flow. So by adjusting the loading distribution, a higher efficiency and more uniform exit flow are expectable, but more specific impacts still need to be discussed.

3. Computational Methodology

3.1. Impeller model

Table 1 shows some typical design parameters of this impeller. Because of a relative high load coefficient, the impeller is almost radial at its exit and the metal angle is around 5°. Besides, the relative Mach number at impeller inlet tip is about 1.12, which means the effect of shockwaves cannot be ignored.

3.2. CFD method

The commercial CFD code NUMECA FINE/Turbo was used to simulate the flow. Spalart–Allmaras model was selected for turbulence calculation. The flow model showed in figure 1 includes a radial and an axial diffuser after the impeller. Both the inlet and outlet domain were extended to ensure the convergence of the calculation. The total pressure(156486Pa) and total temperature(336.94K) are set at inlet and a static pressure are set at outlet as boundary conditions. Adiabatic non-slip wall condition was adopted.

Table 1. Typical parameters of impeller

Parameter	Value
Revolution	n=22000rpm
Flow rate	m=13.53kg/s
Total pressure ratio	Pr=4.0
Inlet tip diameter	$D_0 = 0.282m$
Outlet diameter	$D_2 = 0.4m$
Flow coefficient	$\varphi = 0.127$
Load coefficient	$\phi = 0.875$
Specific speed	0.42

The grid independence was checked and the results are showed in figure 2(solid lines represent total pressure ratio, dashed lines refer to efficiency). The number of grid is around 1.2 million, which have been proved to be meaningful since doubling the number of grid hardly changes the stage performance.

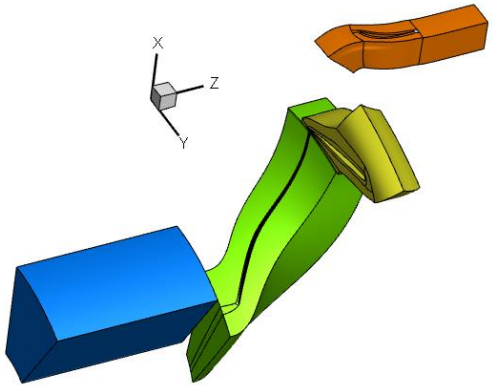


Figure 1. Numerical model

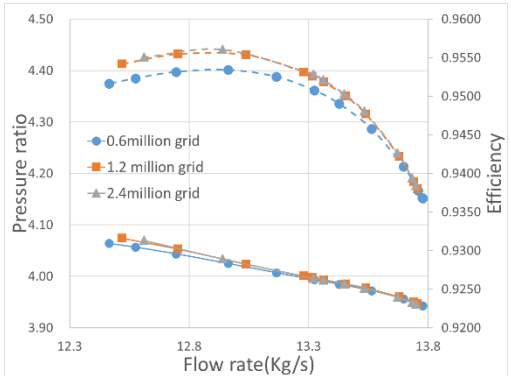


Figure 2. Grid independence validation

4. Results and discussions

4.1. Baseline impellers

Since lots of previous work has proved that an aft-loading at hub leads to a higher efficiency for the impeller, the v_ur distribution at hub were kept a aft-loaded way. But two different degrees of increased v_ur were chosen to compare the performance. However, due to the relatively high loading coefficient of the impeller, the fore-loaded pattern of v_ur may lead to forward-bent at the middle part, so all of the given distributions of v_ur are aft-loaded. The v_ur distributions of two baseline impellers and their performance are showed in figure 3 and figure 4.

As a result, the baseline2 impeller, which is based on a higher v_ur than baseline1 along the flow path, gains a 1.8% higher total pressure ratio and 1.36% higher efficiency at design flow rate. This proves that an increase of v_ur at tip than hub makes a positive influence on the performance, but whether the increase of v_ur at different streamwise location affects impeller performance the same way remains a question. Some further work has been done to address it.

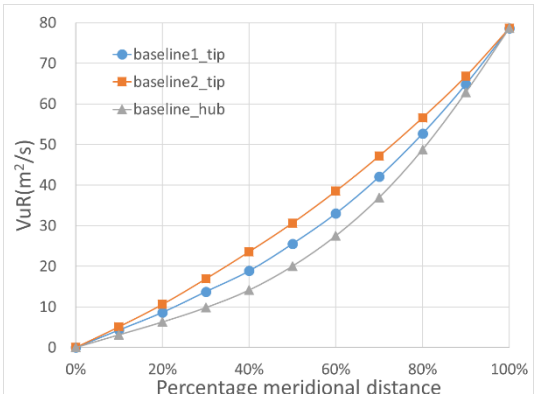


Figure 3. Blade v_ur distributions

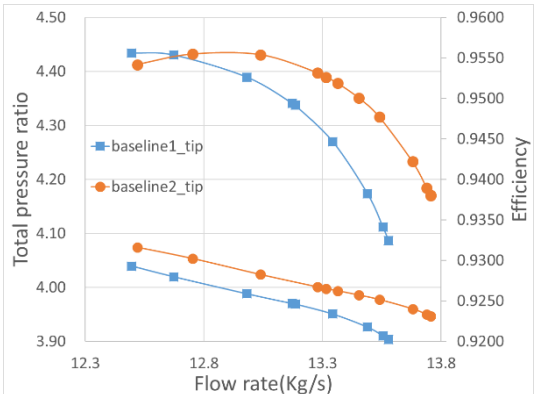


Figure 4. Impeller total pressure ratio and efficiency

4.2. The effect of higher load at the fore part of tip

Figure 5 shows three kinds of v_ur distributions with different degrees of increase at the fore part of tip. As shown in figure 6(solid lines represent total pressure ratio, dashed lines refer to efficiency), the total pressure ratio keeps almost the same in these impellers, while the flow rate of peak efficiency shifts as v_ur increases. A 0.6% higher efficiency can be found at the design flow rate. Efficiency at low flow rate reduces and a narrower surge margin can be found when adding the load.

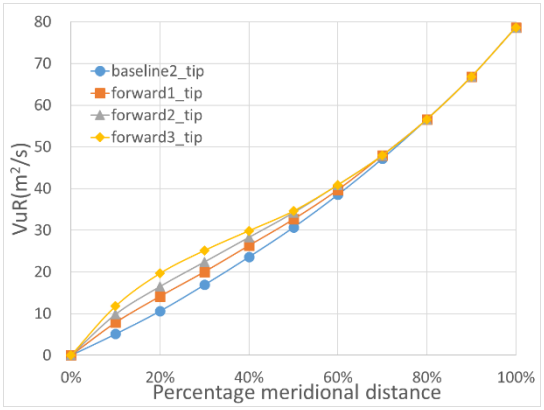


Figure 5. Blade v_ur distributions

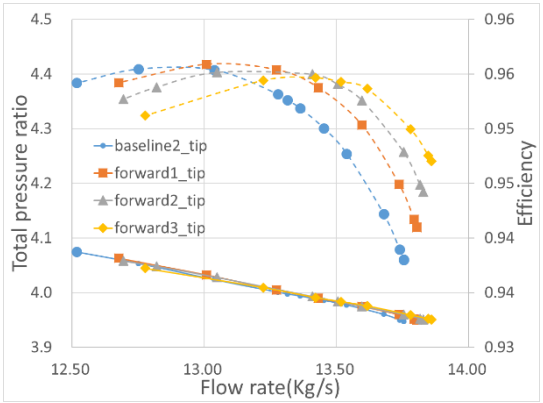


Figure 6. Total pressure ratio and efficiency

The phenomenon can be explained that by increasing the load at fore part at tip, a higher gradient of static pressure is developed from hub to tip on the suction surface of blades, thus suppressing the secondary flow.

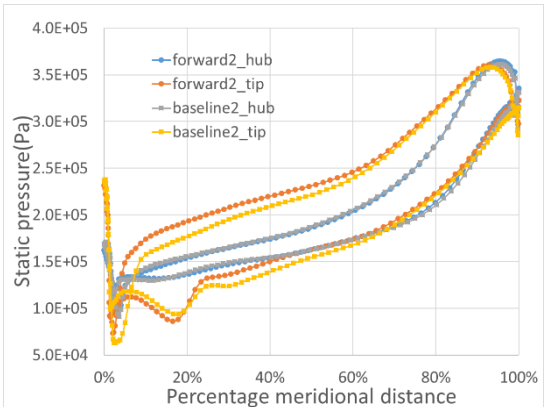


Figure 7. Blade static pressure distributions

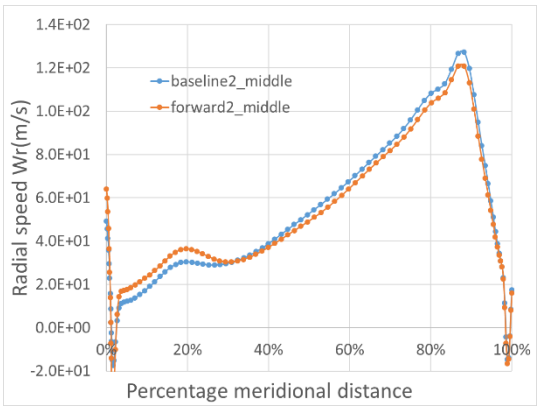


Figure 8. Suction side radial speed distributions

Figure 7 shows the static pressure distribution at 90% and 10% pitchwise for baseline2 and forward2 blades at design flow rate. The static pressure keeps the same at hub, while it rises at tip from 25% to 70% non-dimensional streamwise distance. And a decreased migration speed can be found in the same region from figure 8. The data are extracted from the first layer mesh on the suction surface of blade at 50% pitchwise height. It shows the streamwise distribution of radial component of relative velocity w_r. A positive correlation can be found between the w_r and static pressure gradient from hub to tip. At the fore part of the blade, the static pressure at tip decreases, and the w_r increases as well. However, from the 30% to 90% streamwise distance, the w_r drops with the increase of tip static pressure.

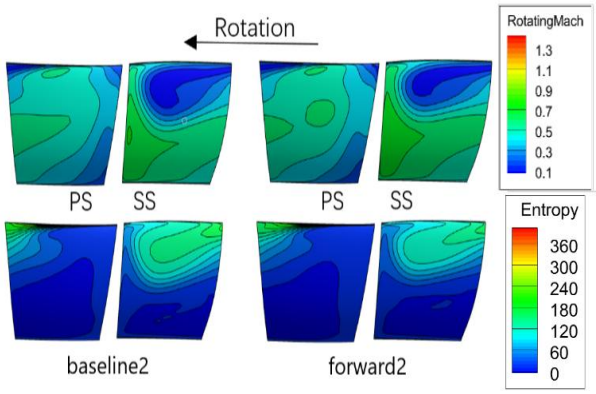


Figure 9. Mach and entropy distributions at impeller outlet

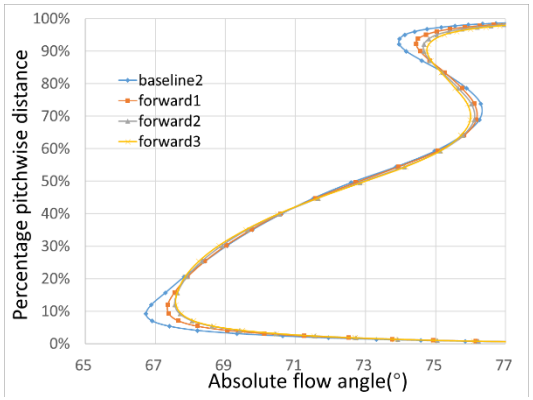


Figure 10. Absolute flow angle distribution

The effect of higher load at fore part of tip can also be proved by the relative Mach and entropy distribution at the exit of different impellers. From figure 9, in the suction surface/shroud corner, a significantly reduced low relative Mach region which are generated by secondary flow can be observed. The entropy in this region reduces as well. And a more uniform impeller exit flow condition can be found in figure 10, which shows the pitchwise distribution of absolute flow angle β for each impeller. Ignoring the relatively high β in the boundary layers close to hub and shroud, a parameter δβ is defined as the difference between the maximum β at around 70% pitchwise distance and the minimum β at around 10% pitchwise distance to present the homogeneity of the exit flow. The δβ reduced 1.2°(relatively 12.6%)in forward2 compared with baseline2.

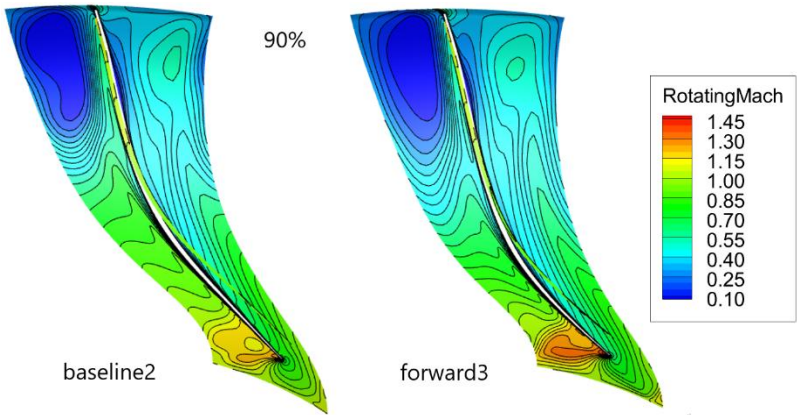


Figure 11. Relative Mach distribution at 90% pitchwise height

On the other side, the increasing load also lead to a large blade curvature at the fore part at tip, where a stronger shock wave is generated. Flow behind this shock are more likely to be separated because of the interaction between shock waves and boundary layer, especially when the flow rate is relatively low. So the surge margin is narrowed by a higher load at the fore part of tip. Figure 11

shows the relative Mach distribution of 90% pitchwise for baseline2 and forward3 impellers at a same flow rate near surge. A larger region of low relative Mach is generated as increasing the load.

4.3. The effect of higher load at the aft part of tip

In this part, three kinds of v_ur distributions with different degrees of increase at the aft part of tip were carried out to obtain the effect. The v_ur distributions and impeller performance are presented in figure 12 and figure 13(solid lines represent total pressure ratio, dashed lines refer to efficiency).

It can be concluded that the total pressure ratio rises when adding the load at the aft part of tip. At the same time, the efficiency curvature becomes gentle. The efficiency rises at high flow rate and slightly declines at low flow rate. Comparing the backward3 with baseline1 impeller, the total pressure ratio rises by 2.3%, the efficiency rises by 0.5% at design flow rate. Notably the flow rate near surge stays almost the same.

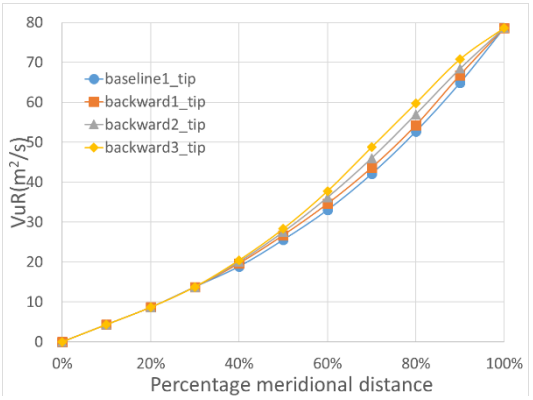


Figure 12. Blade v_ur distributions

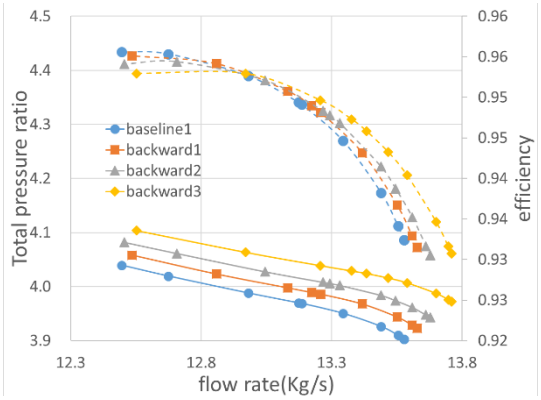


Figure 13. Total pressure ratio and efficiency

Figure 14 shows the static pressure distribution at 90% and 10% pitchwise height, and figure 15 shows the w_r distribution at 50% pitchwise height on the suction side for baseline1 and backward3 impellers. Only a slightly increment of static pressure on the suction side of the blade can be found in backward3 impeller compared to baseline1 and the change of w_r still shows an agreement with the change of static pressure. A more uniform outlet flow is obtained because the δβ was reduced by 0.55°. However, the increment of static pressure on the pressure side is higher than it on the suction side. That means a higher total load on the backward3 impeller, which explains the higher total pressure ratio and absolute flow angle at its exit.

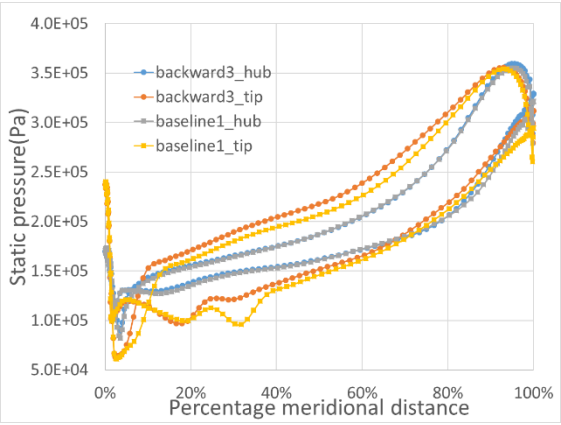


Figure 14. Blade static pressure distributions

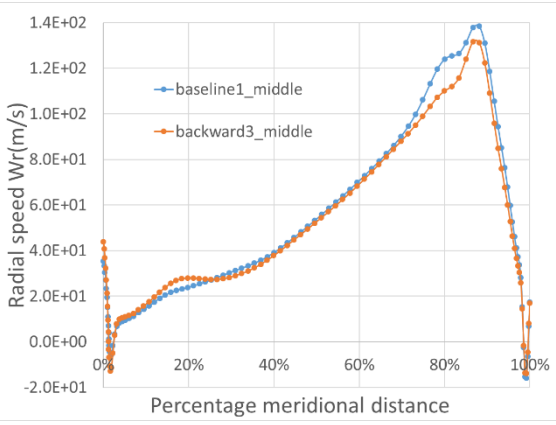


Figure 15. Suction side radial speed distributions

The relative Mach and entropy distribution are also showed in figure 16, and the absolute flow angle at blade exit is presented in figure 17. Since the reduction of high-entropy region is relatively

small, the improvement in efficiency can be caused by both the reduction of secondary flow loss and the increment of input work.

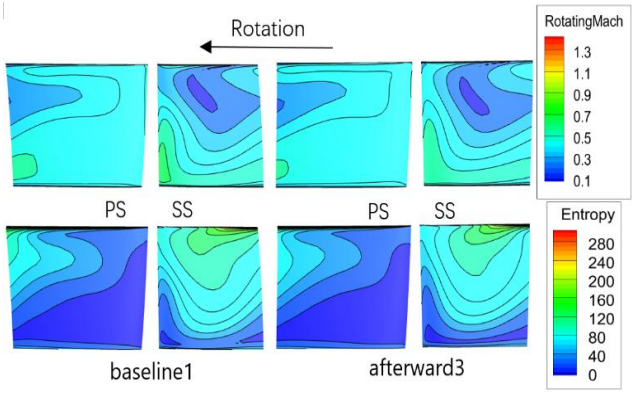


Figure 16. Mach and entropy distributions at impeller outlet

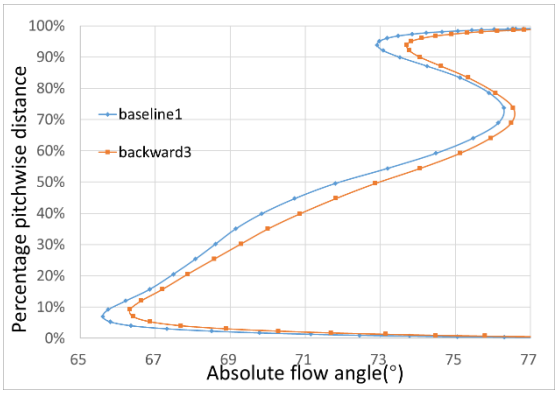


Figure 17. Absolute flow angle distribution

5. Conclusion

In this paper, the numerical calculation of several impellers designed by an inverse method was carried out to investigate the effect of blade tip loading distribution. It was proved that adopting a higher v_ur at tip than hub promotes both the pressure ratio and efficiency of the impeller. but adding v_ur at different streamwise locations at tip affects the impeller performance in diverse ways. From the research, a positive correlation between secondary flow intensity and static pressure gradient from hub to tip on blade surface was established. The numerical calculation result indicates that higher load at the front part promotes the efficiency at design flow rate and improves the uniformity at outlet. However, it decreases the efficiency at low flow rate as well as the surge margin. Higher load at the aft part promotes the total pressure ratio, with no adverse effect on the stable operation range.

References

[1] Zangeneh M, Goto A and Harada H 1998 *J. Journal of Turbomachinery.* **120** 723
[2] Zangeneh M 1998 *Int. Conf. ASME 1998 International Gas Turbine and Aeroengine Congress and Exhibition* vol 1 (Stockholm, Sweden) p V001T01A122
[3] Zangeneh M and Schleer M 2004 *J. Journal of Turbomachinery.* **126** 669
[4] Shi J C, Gao X and Liu B J 2008 *J. Journal of propulsion technology.* **29** 458
[5] Tao L H, Wang J, Liu Y and Liu X 2015 *J. Compressor, Blower & Fan Technology*. **6** 13
[6] Leng H F, Wang F J and Zhang Z C 2013 *Conf. Ser. Mater. Sci. Eng.* **52** 032008
[7] Yagi M, Kishibe T and Shibata T 2008 *Conf. ASME Turbo Expo 2008: Power for Land, Sea, and Air vol 6 (Berlin, Germany)* pp 1639-1648
[8] Ji G F, Yin M X and Gui X M. 2010 *J. Journal of Aerospace Power*. **25** 557